

Thermal conductivity of new nanocomposite superionic semiconductors $K_{0.01}Cu_{1.96}S$, $K_{0.02}Cu_{1.95}S$, $K_{0.03}Cu_{1.94}S$, $K_{0.04}Cu_{1.93}S$, $K_{0.05}Cu_{1.94}S$

M.M. Kubenova^{*,1}, M.Kh. Balapanov², R.Kh. Ishembetov², K.A. Kuterbekov¹, R.F. Almukhametov², K.Zh. Bekmyrza¹, A.M. Kabyshev¹, R.Sh. Palymbetov¹, L.U. Taimuratova³

¹L.N. Gumilyov Eurasian National University, Astana, Kazakhstan

²Ufa University of Science and Technology, Ufa, Russia

³Caspian University of Technology and Engineering named after Sh. Yessenov, Aktau, Kazakhstan

E-mail: kubenova.m@yandex.kz

DOI: 10.32523/ejpfm.2023070307

Received: 21.09.2023 - after revision

In this work, we investigated the effect of nanostructuring on the thermoelectric and thermal properties of nonstoichiometric solid splavs doped with copper sulfides with potassium. The synthesized alloys $K_{0.01}Cu_{1.96}S$, $K_{0.02}Cu_{1.95}S$, $K_{0.03}Cu_{1.94}S$, $K_{0.04}Cu_{1.93}S$, $K_{0.05}Cu_{1.94}S$ are nanocomposite. The crystallite sizes of the synthesized powder, as estimated from the half-width of X-ray diffraction lines, range from 7 to 180 nm. Sample $K_{0.01}Cu_{1.96}S$ is a mixture of phases consisting of chalcocite Cu_2S (82%), jarleite $Cu_{1.96}S$ (12%), anilite $Cu_{1.75}S$ (6%). The composition of samples $K_{0.02}Cu_{1.95}S$ and $K_{0.03}Cu_{1.94}S$ includes the most common phases of copper sulfides - chalcocite Cu_2S , jarleite $Cu_{1.96}S$, digenite $Cu_{1.80}S$. Samples $K_{0.04}Cu_{1.93}S$ and $K_{0.05}Cu_{1.94}S$ consist of jarleite $Cu_{1.96}S$, digenite $Cu_{1.80}S$ and potassium copper sulfide KCu_4S_3 phases. In a practical sense, the extremely low thermal conductivity values (from 0.16 to 0.80 W/m · K) found in the range of 300–700 K for nanocomposite samples $K_{0.02}Cu_{1.95}S$ and $K_{0.03}Cu_{1.94}S$ are very favorable for achieving high thermoelectric figure of merit ZT material.

Keywords: thermal conductivity; nanocomposite; superionic semiconductors

Introduction

In recent years, nanostructuring has been intensively used to increase the thermoelectric figure of merit of thermoelectric materials. In this work, we investigated the effect of nanostructuring on the thermoelectric and thermal properties of nonstoichiometric solid splays doped with copper sulfides with potassium.

Ionic conductors are substances in which electric current is carried out by the movement of ions. The most well-known ionic conductors are liquid electrolytes and molten salts, the electrical conductivity of which can reach $10^2 \text{ Ohm}^{-1}\text{cm}^{-1}$. The flow of current in ionic conductors according to Faraday's law is associated with mass transfer. The electrical conductivity of ionic conductors increases with increasing temperature. Classical ionic crystals of the NaCl type are insulators – at 20°C the conductivity of many of them exceeds $10^{-10} \text{ Ohm}^{-1}\text{cm}^{-1}$ and becomes noticeable only at temperatures close to the melting point [1].

In the 20th century, a new broad class of ionic conductors was discovered – superionic conductors (another term is solid electrolytes), which in the crystalline state have ionic conductivity at the level of liquid electrolytes. The reason for the high mobility of ions in superionic conductors (SIC) is the complete or partial "melting" of one of the crystal sublattices. Ions of the "molten" sublattice can move with a low activation energy (0.10–0.5) eV along a connected network of interstices in the crystalline "framework" formed by the remaining ions.

Both cationic (AgI, $\text{Cu}_4\text{RbCl}_3\text{I}_2$, Li_3N , and others) and anionic SIPs (ZrO_2 , CaF_2 , and others) are known. The current carriers in SIC are cations of silver, copper, sodium, potassium, lithium, zinc, strontium, lead, anions of fluorine, bromine, iodine, oxygen and a number of other ions of both signs. In addition to crystalline SIPs, there are also amorphous ones – glasses, polymers. Superionic conductivity was first discovered in Ag_2S by M. Faraday in 1833. In 1967, the first low-temperature SIC Ag_4RbI_5 with a conductivity of $0.26 \text{ Ohm}^{-1}\text{cm}^{-1}$ for Ag^+ ions was discovered. SIC have been widely used in chemical power sources as solid electrolytes and active electrodes, which has made it possible to increase their shelf life many times and increase the specific energy intensity of batteries and accumulators. Without superionic conductors, modern lithium-ion batteries would not exist. Miniature electrical capacitors (ionistors) with a capacity of hundreds of farads, electrical concentration sensors (for example, determining the oxygen content in the exhaust gases of a car) and others have been created on the basis of SIC.

Silver sulfide still remains the record holder among solids in terms of ionic conductivity – more than $4 \text{ Ohm}^{-1}\text{cm}^{-1}$. Silver and copper chalcogenides ($\text{Ag}_{2+\delta}\text{S}$, $\text{Ag}_{2+\delta}\text{Se}$, $\text{Ag}_{2+\delta}\text{Te}$, $\text{Cu}_{2-\delta}\text{S}$, $\text{Cu}_{2-\delta}\text{Se}$, $\text{Cu}_{2-\delta}\text{Te}$) are mixed electron-ionic conductors (semiconductors), simultaneously possessing high electronic conductivity (from a few to $10^4 \text{ Ohm}^{-1}\text{cm}^{-1}$ depending on the non-stoichiometry δ) and extremely high ionic (cationic) conductivity [1].

Superionic binary copper chalcogenides belong to the so-called self-doped semiconductors. Nonstoichiometric defects, the concentration of which is determined by the nonstoichiometry index δ , play the role of an alloying component (impurity). This impurity forms small levels in the band gap, which are com-

pletely ionized at temperatures from room temperature and above. In uncompensated binary semiconductors, impurity levels can form an impurity band that merges with the main band, which meets the criteria for a heavily doped state [2]. The concentration of impurity carriers n_t electrons in the conduction band and holes in the valence band can be determined by the formula:

$$n_t = \delta N_A / V_m, \quad (1)$$

where N_A is Avogadro's number, $V_m = M / \rho$ is molar volume, M is molar mass, ρ is density.

In the semiconductors under consideration, the concentration of "non-stoichiometric" carriers n_t usually far exceeds the concentration of uncontrolled impurities and equilibrium point defects. The concentration n_i of intrinsic carriers is determined by the temperature and band gap. In most cases, n_i is also significantly less than n_t . In this case, the temperature dependence of electronic conductivity is determined by the temperature dependence of mobility and has a metallic character. In compensated materials with an admixture of monovalent metal M , for example, in solid solutions $(\text{Cu}_{1-x}\text{M}_x)_2\text{X}$ ($\text{X}=\text{S}, \text{Se}, \text{Te}$), the temperature dependence of conductivity is semiconductor in nature.

Nonstoichiometric defects provide high electronic conductivity, which contributes to the high thermoelectric figure of merit of copper chalcogenides [3–7].

In superionic copper chalcogenides, the cations form something like an "ionic liquid" and are highly mobile. This lattice feature results in very low thermal conductivity and consequently high ZT values in this otherwise "simple" semiconductor. This unusual combination of properties makes superionic chalcogenides ideal thermoelectric materials. In [3], a new strategy for searching and creating thermoelectric materials was even formulated, which boils down only to the search for materials with mixed electron-ion conductivity. The appearance of the article [4] caused a real boom in the study of the thermoelectric properties of superionic chalcogenides and the emergence of a whole class of superionic thermoelectrics [8].

A more in-depth analysis of superionic material from the point of view of thermoelectricity was carried out in works [9–10], published earlier than work [3]. "It is known that the maximum thermoelectric figure of merit $ZT = \alpha^2 \sigma T / k \approx 1$ is observed in crystalline semiconductors and semimetals. The value of Z_{max} can be expressed through the characteristic parameters of the substance $N m_d^{3/2} \mu k_L^{-1} T^{3/2} e^r$ if $E_F \ll 1$, or $\approx (m_d / m_c) p^{-2/3} k_L^{-1} T$ if $E_F \gg 1$ (here N – is the number of equivalent extrema in the conduction band (valence band), m_d and m_c – are the effective masses of the density of states and conductivity, μ – is the mobility of current carriers, k_L is the thermal conductivity of the crystal lattice, r and p – are the scattering parameter and concentration of current carriers). The transition from crystalline to disordered amorphous materials reduces the value of Z_{max} due to degradation of the multivalley band structure of the semiconductor (N , $(m_d / m_c \rightarrow 1)$ and a decrease in μ (mode $\lambda = a$, where λ – is the mean free path of current carriers, a – is the interatomic distance)" [9]. The transition to the $\lambda \rightarrow a$ a regime was observed in the disordered paraelectric phase of germanium telluride Ge_{1-x}Te ($T > T_c = 700$ K), the superionic phase of copper

selenide Cu_{2-x}Se ($T > T_c = 430\text{ K}$) [9], as well as in quasicrystals [11], and at the initial stages of this transition, an excessive increase in Z was noted [10].

To explain the growth of Z during the transition $\lambda \rightarrow a$ M.A. Korzhuev used a two-channel model that takes into account the "band" ($\lambda > a$) and diffusion ($\lambda = a$) conduction channels. According to the calculations, the excess growth (Z) is explained by the contribution of the diffusion conduction channel to the kinetic coefficients of the semiconductor.

Experimental part

Nanocomposite copper sulfides $\text{K}_x\text{Cu}_{2-y}\text{S}$ obtained by the liquid-phase synthesis method were chosen as samples for the study. The synthesis reaction is carried out in a melt of hydroxides NaOH and KOH. It is known that the melting point of pure NaOH is 323°C , and for KOH the melting point is 404°C . When the quantitative ratio between NaOH/KOH=51.5: 48.5, the melting point of the mixture decreases to 165°C .

Work is carried out in a fume hood with a coating that is resistant to heated alkalis. The fume hood must be equipped with a forced ventilation system.

First, the prepared mixture of sodium and potassium hydroxides in the same ratio is placed in a Teflon vessel and heated until melting (approximately 165°C). On top, Teflon is surrounded by a stainless steel metal case for strength. The metal also serves to improve the uniformity of heating throughout the entire volume. The lid of the vessel should not be tight so that excess vapor can freely escape from the vessel. After boiling, the heater power is reduced to a minimum to avoid violent boiling. It is recommended to work with protective gloves.

All reagents (CuCl , KCl , $\text{Na}_2\text{S} \cdot 9\text{H}_2\text{O}$) are placed in a heated Teflon vessel at the same time. After filling the charge, the vessel is filled with argon and tightly closed with a threaded lid. In the first half hour, it is recommended to stir the solution, which can be replaced by vibration or shaking.

The $\text{K}_x\text{Cu}_{2-y}\text{S}$ nanostructure is formed within several hours, usually maintained for 15 hours. The sizes of nanocrystallites can be varied by adding a small amount of water to the melt. The product obtained in the form of a clot is washed three times with heated distilled water, then washed with pure ethanol, and dried at room temperature. To isolate individual particle size fractions, the method of sedimentation in a column with alcohol is used.

X-ray diffraction studies of powder samples were carried out using a SmartLab X-ray diffractometer manufactured by Rigaku Corporation. CuK_α radiation ($\lambda = 1.54059\text{ \AA}$) was used. The tube current and voltage were 50 mA and 40 kV, respectively. A one-dimensional detector (D/teX Ultra, Rigaku) with a K_β filter was used, and measurements were taken using a step-scan method over the angle range $2\theta = 10\text{--}80^\circ$, with step ($\Delta 2\theta$) = 0.05° and scan rate = $2^\circ/\text{min}$.

To identify phases and study the crystal structure, PDXL software was used: INTEGRATED X-RAY POWDER DIFFRACTION SOFTWARE and the international ICDD PDF-2 database. The crystallite size was estimated from the half-width of the X-ray lines using the Scherrer formula:

$$D_{hkl} = \frac{K\lambda}{\beta_{hkl}\cos(\theta_{hkl})}, \quad (2)$$

where h, k, l are Miller indices, D_{hkl} – average crystallite size, K – Scherrer coefficient, λ – x-ray wavelength, $2\theta_{hkl}$ – position of the diffraction reflection (hkl), β_{hkl} is the width at half maximum of the diffraction reflection (hkl).

Thermal conductivity measurements were carried out using the flash method on an LFA 467 HT HyperFlash device (NETZSCH, Germany). Thermal conductivity (k) was found from three measurements:

$$k(T) = a(T) \cdot \rho(T) \cdot c_p(T), \quad (3)$$

where T – is temperature, k – is thermal conductivity, a – is thermal diffusivity, ρ – is bulk density, c_p – is specific heat capacity.

Thermal diffusivity was determined using an LFA 467 HT installation using the Parker formula from an analysis of the time dependence of the temperature of the opposite side of the sample after short-term heating of one side of the sample with a powerful light pulse. The heat capacity c_p values were measured on a DSC calorimeter DSC 404 F1 Pegasus (NETZSCH, Germany) in an argon atmosphere. The sample density ρ was found from weight and volume measurements. The error in thermal conductivity measurements did not exceed 10%.

Results and discussion

Figures 1–5 show the results of X-ray phase analysis at room temperature of synthesized nanocomposite copper sulfides $K_xCu_{2-y}S$ with various variations of potassium dopant (0.01, 0.02, 0.03, 0.04, 0.05). The general dynamics of changes in X-ray diffraction patterns depending on the doping impurity concentration indicates that during doping, changes in the crystal lattice occur, accompanied by partial replacement of copper atoms with potassium atoms. Sample $K_{0.01}Cu_{1.96}S$ is a mixture of phases consisting of chalcocite Cu_2S (82%), jarleite $Cu_{1.96}S$ (12%), anilite $Cu_{1.75}S$ (6%). Samples $K_{0.04}Cu_{1.93}S$ and $K_{0.05}Cu_{1.94}S$ consist of the phases of jarleite $Cu_{1.96}S$, digenite $Cu_{1.80}S$ and potassium copper sulfide KCu_4S_3 [12]. The composition of samples $K_{0.02}Cu_{1.95}S$ and $K_{0.03}Cu_{1.94}S$ includes the most common phases of copper sulfides – chalcocite Cu_2S , jarleyite $Cu_{1.96}S$, digenite $Cu_{1.80}S$, which is in good agreement with several sets of data from the literature [13–15].

Since the cubic phase of Cu_2S is usually stable at temperatures above $435^\circ C$ [16], we believe that the presence of this phase can be explained by the fact that potassium is partially incorporated into the cubic lattice of Cu_2S and has a stabilizing effect, making the structure stable at room temperature. Another possible explanation is that in nanomaterials, as particle sizes decrease, the temperatures of polymorphic transformations change, metastable states are fixed, or phases are formed that are not at all characteristic of the bulk state [17]. Based on estimates from the half-width of X-ray lines, the sizes of crystallites in the alloy range from 7 to 180 nm.

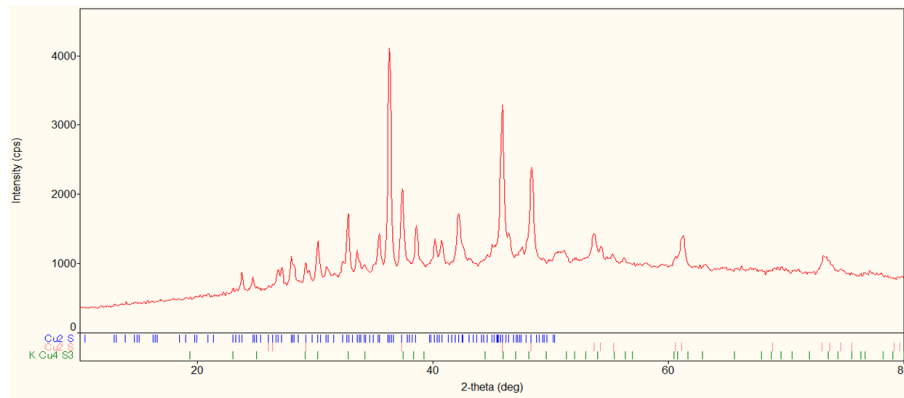


Figure 1. X-ray diffraction spectrum of the $K_{0.01}Cu_{1.96}S$ sample at room temperature.

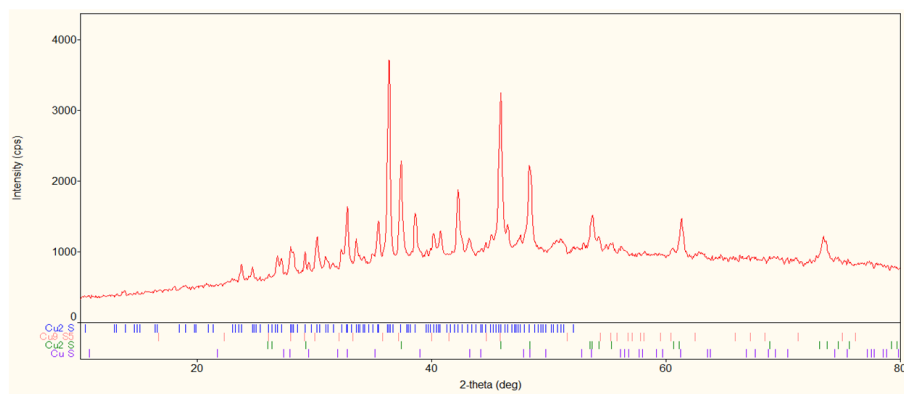


Figure 2. X-ray diffraction spectrum of the $K_{0.02}Cu_{1.95}S$ sample at room temperature.

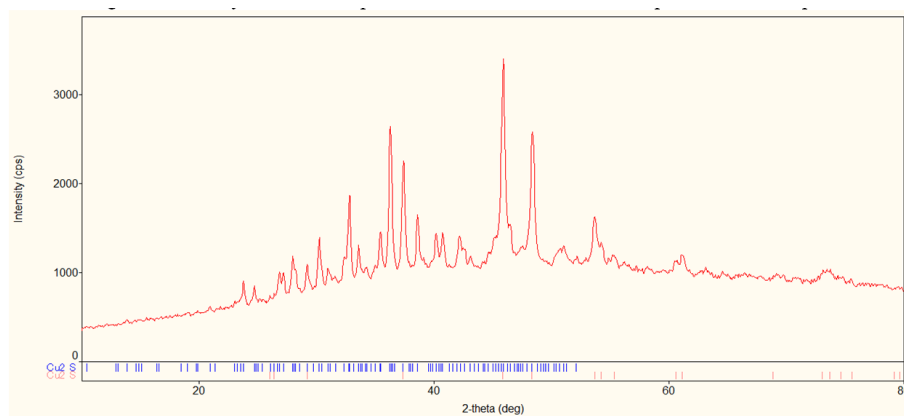


Figure 3. X-ray diffraction spectrum of the $K_{0.03}Cu_{1.94}S$ sample at room temperature.

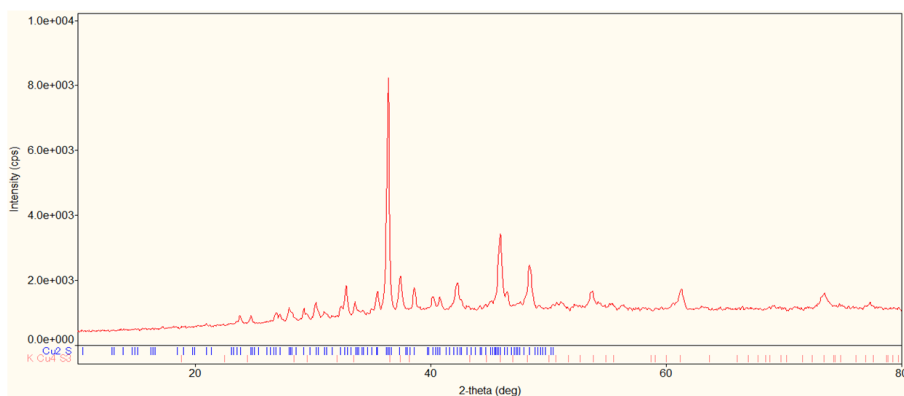


Figure 4. X-ray diffraction spectrum of the $K_{0.04}Cu_{1.93}S$ sample at room temperature.

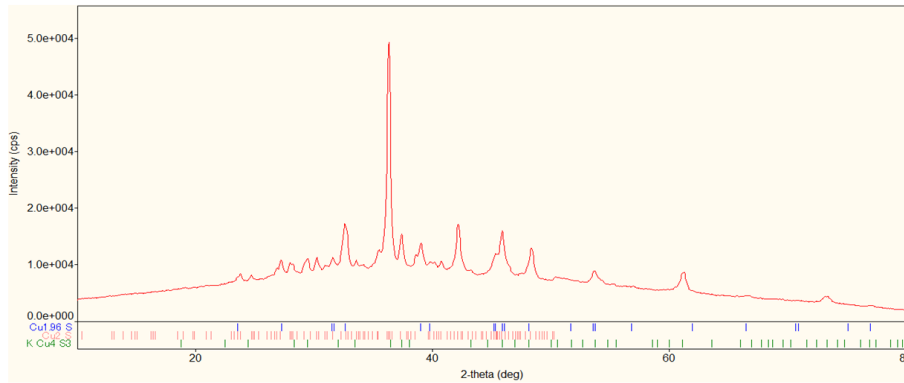


Figure 5. X-ray diffraction spectrum of the $K_{0.05}Cu_{1.94}S$ sample at room temperature.

The cubic and hexagonal phases of digenite and chalcocite are superionic [18]. Consequently, the studied $K_{0.01}Cu_{1.96}S$, $K_{0.02}Cu_{1.95}S$, $K_{0.03}Cu_{1.94}S$, $K_{0.04}Cu_{1.93}S$, $K_{0.05}Cu_{1.94}S$, in which these two phases predominate according to X-ray phase analysis, should exhibit superionic properties, at least above temperatures of 380–400 K. DSC calorimetry revealed a strong thermal effect of about 378 K for all samples, which corresponds to a high content of the monoclinic chalcocite phase in the alloys [19].

The mobile cations in copper sulfide can be likened to a "cationic liquid" that fills the voids of the structure. The presence of a "liquid-like phase" inside a "solid" lattice interferes with the normal propagation of phonons ("phonon glass" materials) [20], therefore superionic copper chalcogenides have low lattice thermal conductivity. Additional factors reducing the overall thermal conductivity are impurity potassium ions, leading to an increase in the scattering of phonons and electrons, as well as the nanodispersity of grains, which increases the number of structural defects at phase boundaries.

Figure 6 shows the results of measuring the total thermal conductivity of samples in the temperature range from room temperature to 700 K.

As a consequence of the disordering of the crystal lattice, the thermal conductivity coefficients of the alloys $K_{0.01}Cu_{1.96}S$, $K_{0.02}Cu_{1.95}S$, $K_{0.03}Cu_{1.94}S$, $K_{0.04}Cu_{1.93}S$, $K_{0.05}Cu_{1.94}S$ in the studied temperature range have low values in the range (0.09–6.29 W/m · K), which can be seen in Figure 6. The decrease in thermal conductivity with increasing temperature can be explained by a decrease in the electronic component of thermal conductivity. The decrease in thermal conductivity is associated with a decrease in the rate of passage of phonons during partial "melting" of the lattice, which occurs during the transition of the material to the superionic state.

The $K_{0.03}Cu_{1.94}S$ sample has the lowest thermal conductivity. Its thermal conductivity does not exceed 0.71 W/m · K, dropping to 0.17 W/m · K. Similar thermal properties are exhibited by a sample of composition $K_{0.02}Cu_{1.95}S$, the thermal conductivity of which lies in the range from 0.16 to 0.80 W/m · K. Above 670 K, the lowest thermal conductivity among all studied samples is shown by the $K_{0.04}Cu_{1.93}S$ nanocomposite (0.09–0.16 W/m · K). The thermal conductivity of the $K_{0.05}Cu_{1.94}S$ sample is the highest among the studied compositions; it rises to 6.3 W/m · K at a phase transition of about 390 K and does not fall below

1 W/m · K.

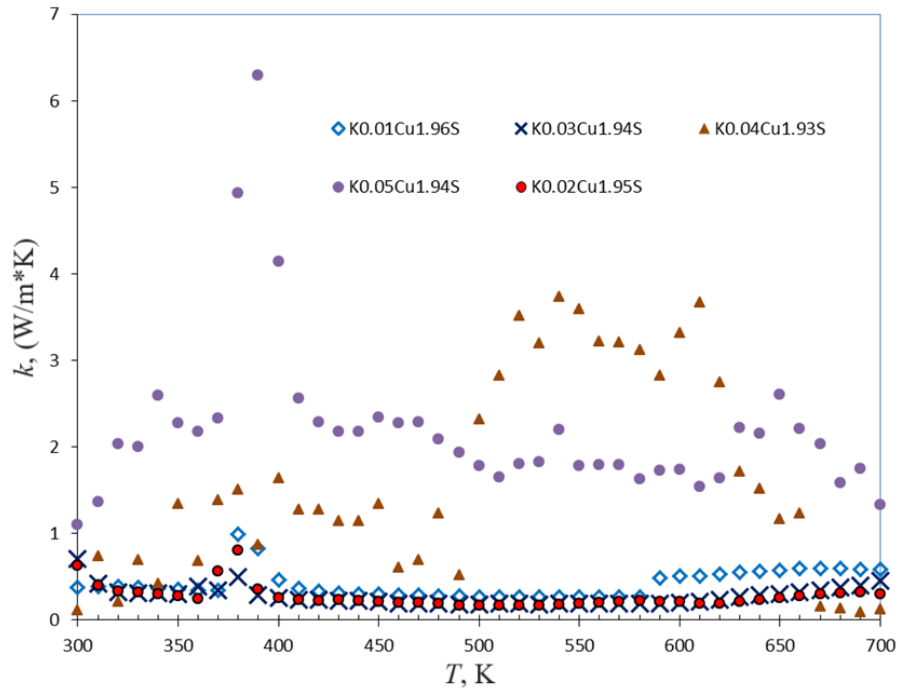


Figure 6. Temperature dependence of the thermal conductivity coefficient of the alloys $K_{0.01}Cu_{1.96}S$, $K_{0.02}Cu_{1.95}S$, $K_{0.03}Cu_{1.94}S$, $K_{0.04}Cu_{1.93}S$, $K_{0.05}Cu_{1.94}S$.

The value of the dimensionless thermoelectric figure of merit ZT , which characterizes the operating efficiency of thermoelectric materials in thermoelectric devices, is determined by the formula:

$$ZT = a^2\sigma T/k, \quad (4)$$

where a – is the Seebeck coefficient; σ – conductivity; k – is the thermal conductivity of the material. Thus, low thermal conductivity favors a high thermoelectric figure of merit of the material. However, the ZT value depends on three interrelated parameters, so optimizing the material composition to achieve the highest ZT is a very difficult task.

It is known that coulometric titration in a cell of the $Cu/CuBr/K_yCu_{2-x-y}S$ / type allows the controlled introduction and removal of copper from a superionic sample, controlling its nonstoichiometry and properties. This makes copper and silver chalcogenides convenient model systems for optimizing their physical properties, and, in particular, thermoelectric figure of merit. Recently, for a similar $K_{0.04}Cu_{1.85}S$ nanocomposite based on non-stoichiometric copper sulfide, our laboratory obtained an extremely high thermoelectric figure of merit $ZT = 9.67$ at a temperature of 605 K [21], which was achieved with a thermal conductivity of about 0.2 W/m · K.

Conclusion

The synthesized alloys $K_{0.01}Cu_{1.96}S$, $K_{0.02}Cu_{1.95}S$, $K_{0.03}Cu_{1.94}S$, $K_{0.04}Cu_{1.93}S$, $K_{0.05}Cu_{1.94}S$ are nanocomposite. The crystallite sizes of the synthesized powder,

as estimated from the half-width of X-ray diffraction lines, range from 7 to 180 nm. Sample $K_{0.01}Cu_{1.96}S$ is a mixture of phases consisting of chalcocite Cu_2S (82%), jarlite $Cu_{1.96}S$ (12%), anilite $Cu_{1.75}S$ (6%). The composition of samples $K_{0.02}Cu_{1.95}S$ and $K_{0.03}Cu_{1.94}S$ includes the most common phases of copper sulfides - chalcocite Cu_2S , jarlite $Cu_{1.96}S$, digenite $Cu_{1.80}S$. Samples $K_{0.04}Cu_{1.93}S$ and $K_{0.05}Cu_{1.94}S$ consist of jarlite $Cu_{1.96}S$, digenite $Cu_{1.80}S$ and potassium copper sulfide KCu_4S_3 phases.

The $K_{0.03}Cu_{1.94}S$ sample has the lowest thermal conductivity in the range of 300–700 K. Its thermal conductivity does not exceed $0.71 \text{ W/m} \cdot \text{K}$, dropping to $0.17 \text{ W/m} \cdot \text{K}$. Similar thermal properties are exhibited by a sample of composition $K_{0.02}Cu_{1.95}S$, the thermal conductivity of which lies in the range from 0.16 to $0.80 \text{ W/m} \cdot \text{K}$. However, above 670 K, the $K_{0.04}Cu_{1.93}S$ nanocomposite shows the lowest thermal conductivity among all the studied samples (0.09 – $0.16 \text{ W/m} \cdot \text{K}$). The thermal conductivity of the $K_{0.05}Cu_{1.94}S$ sample is the highest among the studied compositions; it rises to $6.3 \text{ W/m} \cdot \text{K}$ at a phase transition of about 390 K and does not fall below $1 \text{ W/m} \cdot \text{K}$.

In a practical sense, the extremely low thermal conductivity values (from 0.16 to $0.80 \text{ W/m} \cdot \text{K}$) found in the range of 300–700 K for nanocomposite samples $K_{0.02}Cu_{1.95}S$ and $K_{0.03}Cu_{1.94}S$ are very favorable for achieving high thermoelectric figure of merit ZT material.

Acknowledgments

The Science Committee of the Republic of Kazakhstan, which is part of the Ministry of Science and Higher Education, provided funding for this research (No. AP14871197).

References

- [1] A.K. Ivanov-Schitz and I. V. Murin, *KSolid-State Ionics* (SPbGU, St. Petersburg, 2010), Vol. 2 (in Russian) [[WebLink](#)]
- [2] V.I. Fistul, *Heavily doped semiconductors* (Nauka, Moscow, 1967) 416 p. (in Russian) [[WebLink](#)]
- [3] H. Liu et al., *Nature Materials* **11** (2012) 422–425. [[CrossRef](#)]
- [4] T.W. Day et al., *Materials for Renewable and Sustainable Energy* **3** (2014) 26. [[CrossRef](#)]
- [5] S. Ballikaya et al., *J. Mater. Chem. A* **1** (2013) 12478–12484. [[CrossRef](#)]
- [6] K. Tyagi et al., *J. Phys. Chem. Sol.* **81** (2015) 100–105. [[CrossRef](#)]
- [7] L. Yang et al., *Acta Materialia* **113** (2016) 140–146. [[CrossRef](#)]
- [8] P. Qin et al., *Inorg. Chem. Front.* **4** (2017) 1192–1199. [[CrossRef](#)]
- [9] M.A. Korzhuev, *Physics* **11** (1993) 3043. (In Russian) [[WebLink](#)]
- [10] M.A. Korzhuev, *St. Petersburg: NINP RAS* (2002) 133–138. (In Russian) [[WebLink](#)]
- [11] K. Kiriwara et al., *Journal of Alloys and Compounds* **342** (2002) 469–472. [[CrossRef](#)]

- [12] D.B. Brown et al., *Inorganic Chemistry* **19**(7) (1980), 1945–1950. [[CrossRef](#)]
- [13] S.D. Kang et al., *Materials Today Physics* **1** (2017) 7–13. [[CrossRef](#)]
- [14] Z.H. Ge et al., *Advanced Energy Materials* **6** (2016) 1600607. [[CrossRef](#)]
- [15] M.M. Kubenova et al., *Nanomaterials* **11**(9) (2021) 2238. [[CrossRef](#)]
- [16] N.Kh. Abrikosov et al., *Semiconducting Chalcogenides and Alloys on Their Basis* (Nauka, Moscow, 1975) 220 p. (In Russian)
- [17] I.P. Suzdalev, *Nanotechnology: Physicochemistry of nanoclusters, nanostructures and nanomaterials* (LIBROCOM, Moscow 2009) 592 p. (in Russian)
- [18] M.Kh. Balapanov et al., *Bulletin of the Russian Academy of Sciences. Physics* (2005) **69**(4) 545–548. (In Russian)
- [19] M.Kh. Balapanov et al., *Bulletin of the Bashkir University* **26**(4) (2021) 961–964. (In Russian)
- [20] H.L. Liu et al., *Nat. Mater.* **11** (2012) 422–425. [[CrossRef](#)]
- [21] S.M. Sakhabayeva et al., *Recent Contributions to Physics* **4**(79) (2021) 72–81. [[CrossRef](#)]